

Copyright WILEY-VCH Verlag GmbH & Co. KGaA, 69469 Weinheim, Germany, 2016.



Supporting Information

for *Adv. Energy Mater.*, DOI: 10.1002/aenm.201600322

Integrated Intercalation-Based and Interfacial Sodium Storage
in Graphene-Wrapped Porous Li₄Ti₅O₁₂ Nanofibers Composite
Aerogel

*Chaoji Chen, Henghui Xu, Tengfei Zhou, Zaiping Guo, Lineng
Chen, Mengyu Yan, Liqiang Mai, Pei Hu, Shijie Cheng,
Yunhui Huang,* and Jia Xie**

Supporting information

Integrated Intercalation-Based and Interfacial Sodium Storage in Graphene-Wrapped Porous Li₄Ti₅O₁₂ Nanofibers Composite Aerogel

Chaoji Chen, Henghui Xu, Tengfei Zhou, Zaiping Guo, Lineng Chen, Mengyu Yan, Liqiang Mai, Pei Hu, Shijie Cheng, Yunhui Huang and Jia Xie**

E-mail: xiejia@hust.edu.cn; huangyh@mail.hust.edu.cn

Supplementary method S1: calculation details for the separation of the diffusion-controlled and capacitive-controlled charge contributions

The total current (or charge) of the electrode at a certain potential can be divided into two parts, described as: $i(V) = k_1v^{1/2} + k_2v$ and $i(V)/v^{1/2} = k_1 + k_2v^{1/2}$ (Eq. 1), on the base of the power law relationship of $i = av^{1/2}$ for solid-state diffusion-controlled processes and $i = av$ for non-diffusion limited (capacitive-controlled) processes. The current values at a certain potential can be determined by the cyclic voltammograms at various scan rates of 0.1–100 mV s⁻¹. By plotting curves of $i(V)/v^{1/2}$ vs. $v^{1/2}$ (v varies from 0.1 to 100 mV s⁻¹), the values of k_1 (intercept) and k_2 (slope) at a certain potential can be determined according to Eq. 1. When the series k_1 and k_2 values at different potentials are quantified, the values of $k_1v^{1/2}$ and k_2v at a fixed scan rate (v) can be determined, thus the diffusion-controlled ($k_1v^{1/2}$) and capacitive-controlled (k_2v) currents are separated.

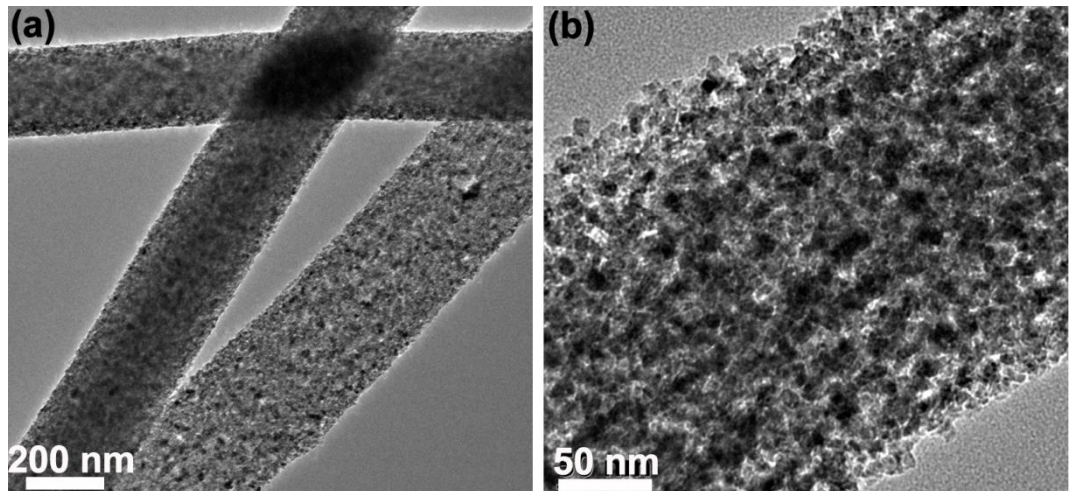


Figure S1. TEM images for the PLTO nanofibers.

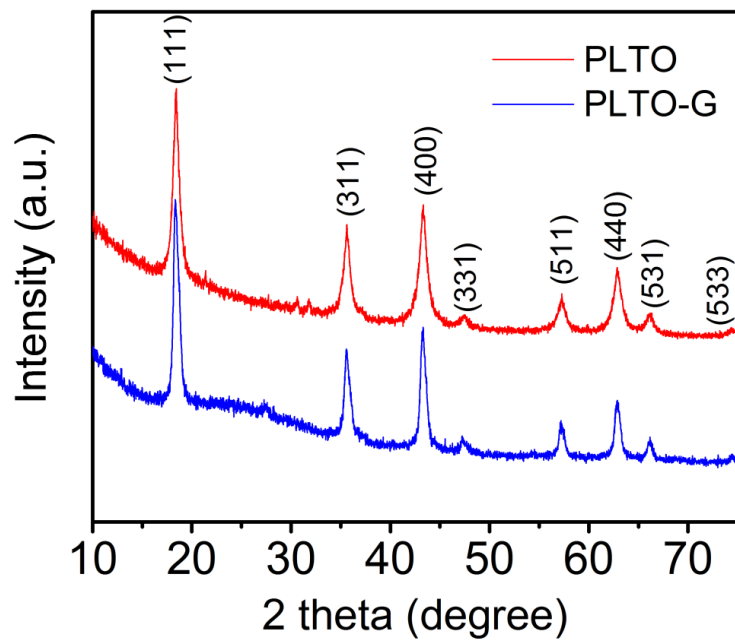


Figure S2. XRD patterns for the PLTO and G-PLTO products.

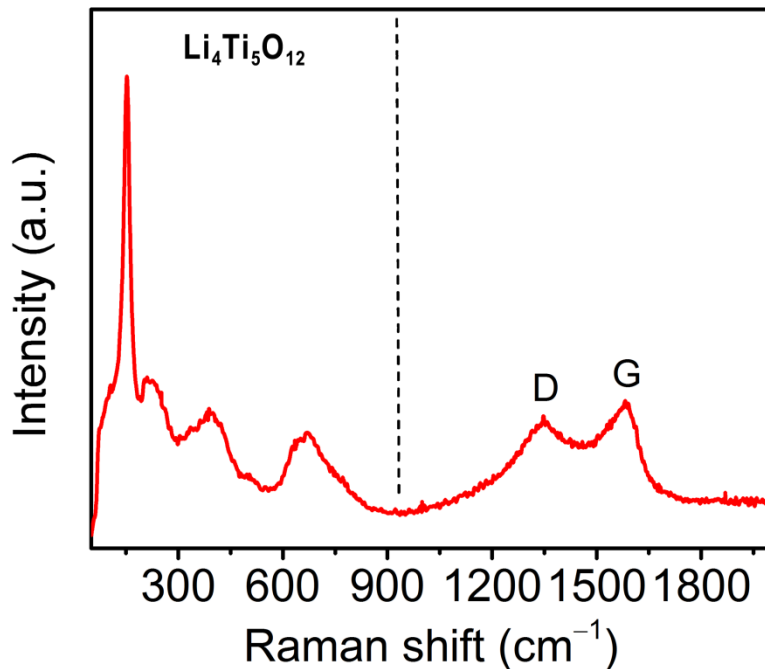


Figure S3. Raman spectrum for the G-PLTO composite aerogel.

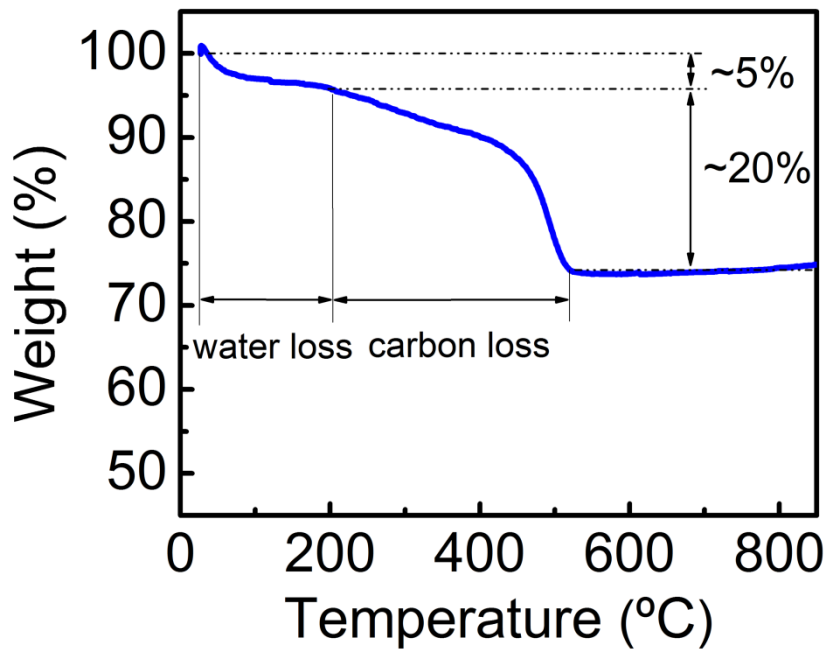


Figure S4. TG curve for the G-PLTO composite aerogel. The carbon content is quantified to ~20% based on the TG measurements.

Table S1. Comparisons of Ti-based, carbon-based and P-based anodes in sodium-ion batteries

	Material name	Safety	Capacity (mAh g ⁻¹)	Cycling durability	Theoretical investigation	Sources
Ti-based anodes	Li ₄ Ti ₄ O ₁₂	good	175 at 0.1C ^a	50	Yes	Ref. 1
	C-coated Li ₄ Ti ₅ O ₁₂	good	160 at 0.5C	50	No	Ref. 2
	Nano-Li ₄ Ti ₄ O ₁₂	good	150 at 0.1C	none	Yes	Ref. 3
	Porous Li ₄ Ti ₅ O ₁₂	good	150 at 0.1C	100	No	Ref. 4
	Na-Doped Li ₄ Ti ₅ O ₁₂	good	160 at 0.1C	800	No	Ref 5
	L ₄ T ₅ O ₁₂ -TiO ₂	good	148 at 1C	400	No	Ref. 6
	C-coated TiO ₂	good	168 at 0.5C	100	No	Ref. 7
	NaTiO ₂	good	150 at 0.1C	50	Yes	Ref. 8
	Carbon/TiO ₂	good	160 at 0.1 C	100	No	Ref. 9
	TiO ₂ @C nanospheres	good	139 at 0.3 C	500	Yes	Ref. 10
Safety: good	TiO ₂ /graphene	good	170 at 1C	4300	Yes	Ref. 11
Capacity: Low	Sodium titanate-CNT	good	100 at 1C	3500	No	Ref. 12
Cyclability: good	NaTi ₂ (PO ₄) ₃ -graphene	good	120 at 0.5C	1000	No	Ref. 13
	TiO ₂ -B	good	145 at 0.1C	75	No	Ref. 14
	C-coated TiO ₂ nanotube	good	170 at 0.1C	70	No	Ref.15
	TiO ₂ -coated NaTi ₂ (PO ₄) ₃	good	96 at 0.2C	10,000	No	Ref. 16
	G-PLTO composite	good	~200 at 0.2C	12,000	Yes	This work
Carbon-based anodes	N-doped carbon fiber	inferior	134 at 200 mA g ⁻¹	200	No	Ref. 17
	N-doped carbon sheets	inferior	190 at 200 mA g ⁻¹	260	No	Ref. 18
	N-doped activated porous carbon fiber	inferior	200 at 200 mA g ⁻¹	100	No	Ref. 19
	N/O-co-doped carbon nanobubbles	inferior	100 at 100 mA g ⁻¹	80	No	Ref. 20
	Carbon nanosheet frameworks	inferior	300 at 50 mA g ⁻¹	200	No	Ref. 21
	Nanocellular carbon foam	inferior	150 at 50 mA g ⁻¹	200	No	Ref. 22
	Sulfur-doped graphene	inferior	280 at 50 mA g ⁻¹	100	No	Ref. 23
	Nitrogen-doped hollow carbon spheres	inferior	220 at 100 mA g ⁻¹	500	No	Ref. 24
Safety: inferior	Nitrogen-doped carbon nanofibers	inferior	280 at 50 mA g ⁻¹	200	No	Ref. 25
Capacity: medium	Nitrogen-containing mesoporous carbons	inferior	220 at 70 mA g ⁻¹	100	No	Ref. 26
Cyclability: medium	Nitrogen-doped carbon sheets	inferior	210 at 100 mA g ⁻¹	600	No	Ref. 27
	Expanded graphite	inferior	91 at 200 mA g ⁻¹	2000	No	Ref. 28
	N/S-codoped carbon microsphere	inferior	280 at 30 mA g ⁻¹	3400	Yes	Ref. 29
P-based anodes	Red P-carbon	medium	1890 at 143 mA g ⁻¹	30	No	Ref. 30
	Amorphous P	medium	1800 at 250 mA g ⁻¹	140	No	Ref. 31
	P-graphene	medium	1700 at 520 mA g ⁻¹	60	No	Ref. 32
	Black P-graphite	medium	1750 at 2.6 A g ⁻¹	100	No	Ref. 33
Safety: medium	P nanoparticle-graphene	medium	2000 at 0.5 A g ⁻¹	150	No	Ref. 34
Capacity: high	Sn ₄ P ₃ -C	medium	850 at 50 mA g ⁻¹	150	No	Ref. 35
Cyclability: inferior	FeP	medium	420 at 50 mA g ⁻¹	40	No	Ref. 36
	SiP	medium	1000 at 120 mA g ⁻¹	35	No	Ref. 37
	Yolk-shell Sn ₄ P ₃ @C	medium	650 at 200 mA g ⁻¹	400	No	Ref. 38

^a 1C = 175 mA g⁻¹

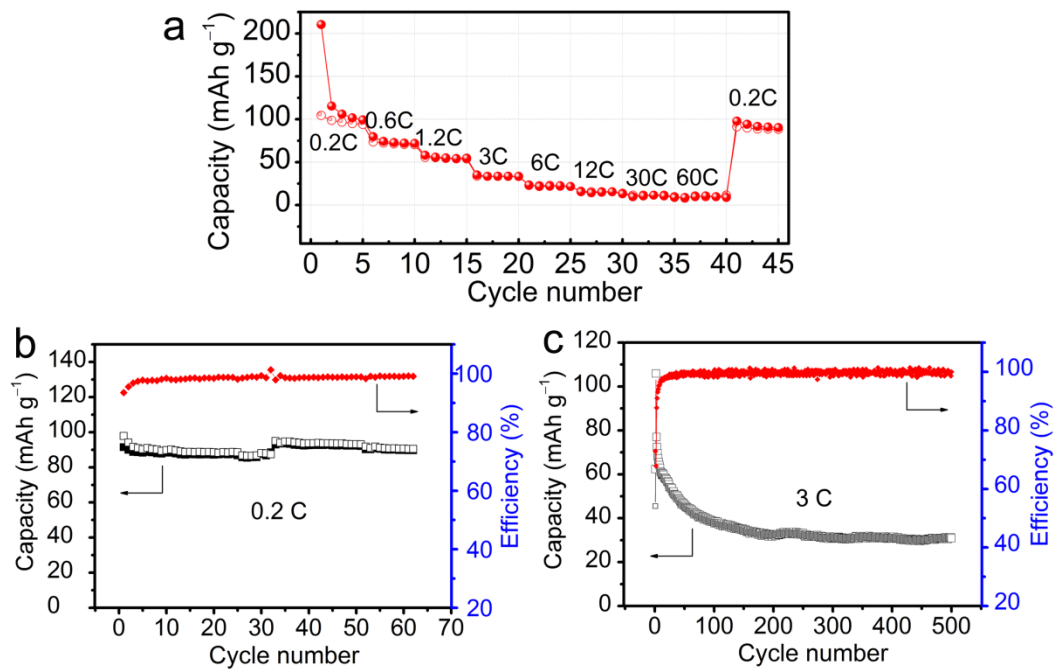


Figure S5. Sodium storage performance of the PLTO electrode: (a) rate performance at various C-rates, (b) cycling performance at 0.2 C after the rate performance test in a, and (c) long-term cycling performance at 3 C for 500 cycles.

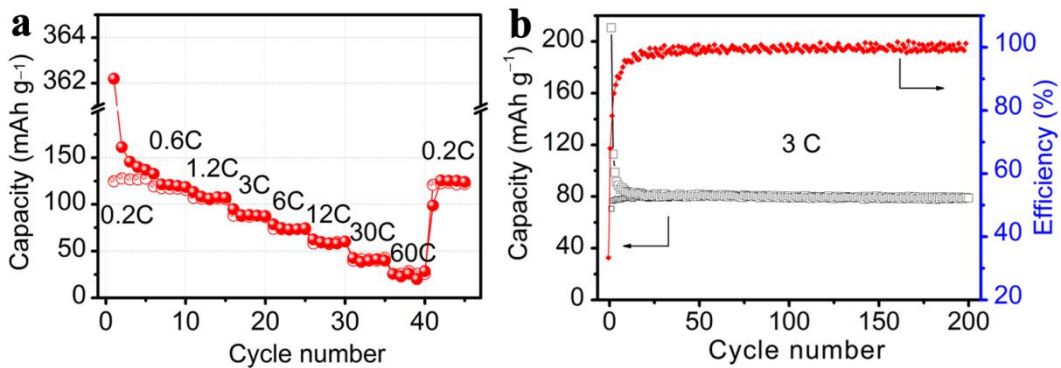


Figure S6. Sodium storage performance of the GA (graphene aerogel) electrode: (a) rate performance at various C-rates, (b) cycling performance at 3 C for 200 cycles (1 C = 175 mA g⁻¹).

The capacity of the G-PLTO composite aerogel is contributed by two components: the graphene framework and the PLTO nanofibers, as described as:

$$C_{(\text{G-PLTO composite aerogel})} = 0.2*C_{(\text{graphene in the composite})} + 0.8*C_{(\text{PLTO in the composite})} \quad (\text{Eq. 2}).$$

Assuming that the capacity values of the graphene framework in the G-PLTO composite are the same as the graphene aerogel in Figure S6a, the capacity contributions of the graphene framework in the composite at various C-rates can be calculated by $0.2*C_{(\text{graphene in the composite})}$, demonstrated by 30, 24, 22, 18, 15, 11.6, 7 and 5 mA h g⁻¹ at 0.2, 0.6, 1.2, 3, 6, 12, 30, and 60 C, respectively (see Table S2). As the capacity values of the G-PLTO composite have also been determined (Figure 4a), the capacity contributions of the PLTO nanofibers can be quantified by $0.8*C_{(\text{PLTO in the composite})} = C_{(\text{G-PLTO composite aerogel})} - 0.2*C_{(\text{graphene in the composite})}$ according to Eq. 2, as listed in Table S2. Based on the above analysis, the capacities delivered by the PLTO nanofibers in the composite (that is, capacities calculated basing on the PLTO

nanofibers) can be determined as $C_{(\text{PLTO in the composite})} = [C_{(\text{G-PLTO composite aerogel})} - 0.2*C_{(\text{graphene in the composite})}]/0.8$, demonstrated by 212.5, 195, 153.75, 121.35, 81.25, 58, 41.25 and 37.5 mA h g⁻¹ at 0.2, 0.6, 1.2, 3, 6, 12, 30, and 60 C, respectively. Therefore, we can conclude that the capacity of the G-PLTO composite is mainly contributed by the PLTO nanofibers with minor from the graphene frameworks.

Table S2. Capacity contributions from the graphene and PLTO components in the G-PLTO composite aerogel (unit: mA h g⁻¹, 1 C = 175 mA g⁻¹)

Contribution\ C-rate	0.2C	0.6C	1.2C	3C	6C	12C	30C	60C
$C_{(\text{G-PLTO composite aerogel})}$	200	180	145	115	80	58	40	35
$C_{(\text{graphene in the composite})}$	150	120	110	90	75	58	35	25
$0.2*C_{(\text{graphene in the composite})}$	30	24	22	18	15	11.6	7	5
$C_{(\text{PLTO in the composite})}$	212.5	195	153.75	121.25	81.25	58	41.25	37.5
$0.8*C_{(\text{PLTO in the composite})}$	170	156	123	97	65	46.4	33	30

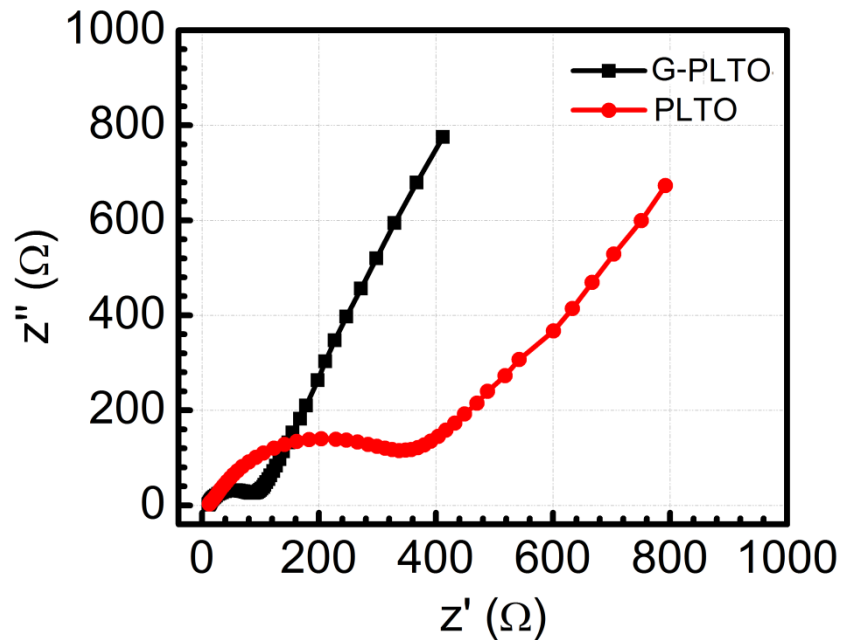


Figure S7. EIS spectra for the G-PLTO and PLTO electrodes.

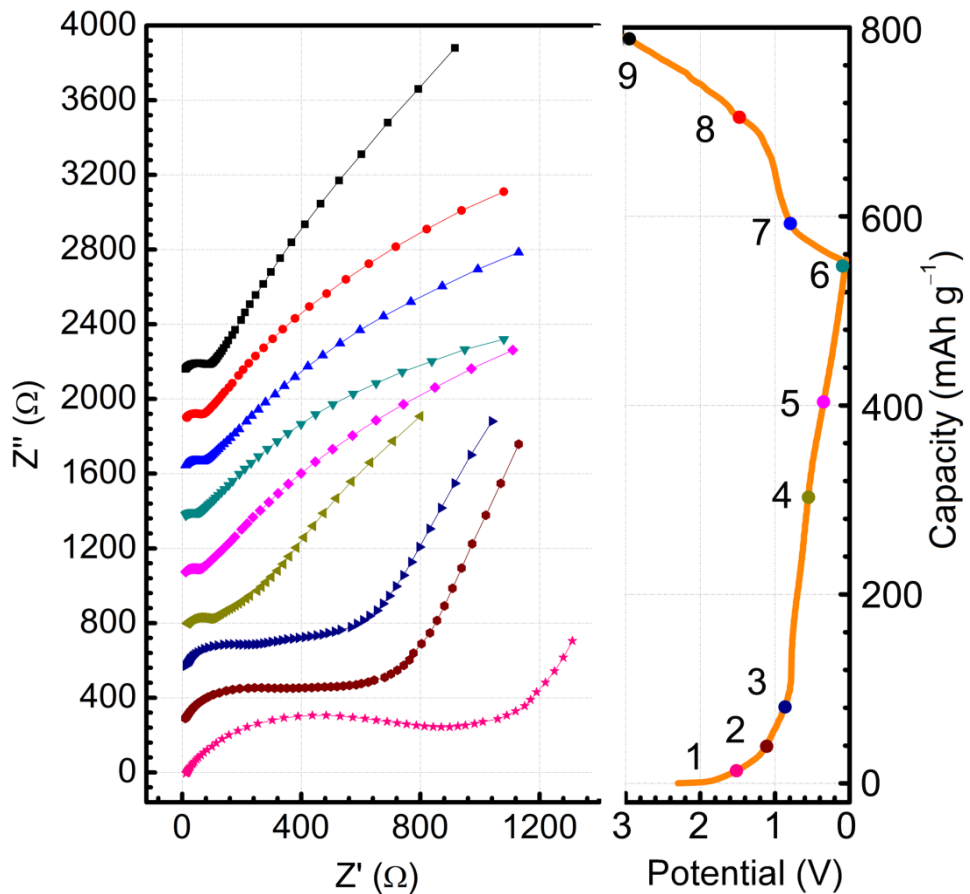


Figure S8. *In-situ* EIS spectra for the G-PLTO electrodes during the initial discharge-charge cycle at a current rate of 0.2 C.

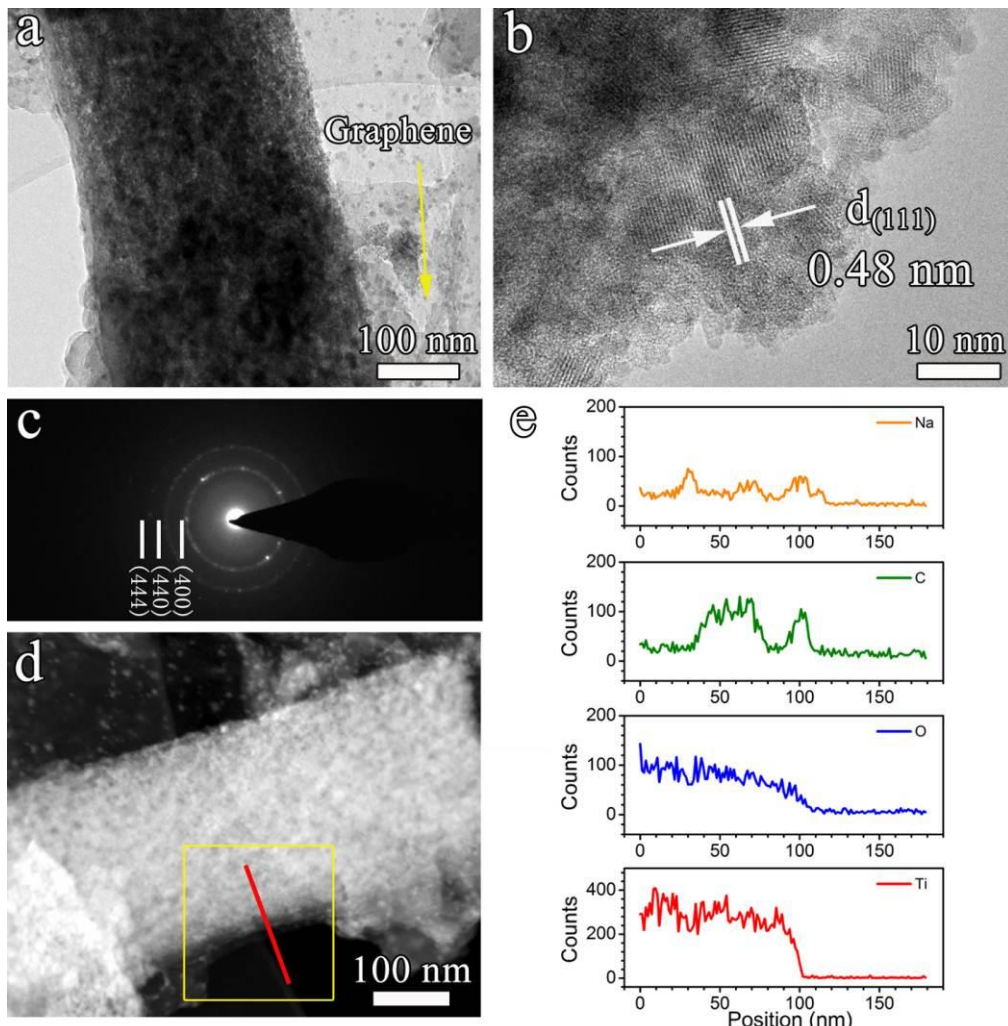


Figure S9. Structure stability of the G-PLTO electrode after 10,000 discharging-charging cycles: (a) TEM image, (b) HR-TEM image, (c) SAED pattern, (d) STEM image and (e) the corresponding EDX spectra.

References

- [1] Y. Sun, L. Zhao, H. Pan, X. Lu, L. Gu, Y. Hu, H. Li, M. Armand, Y. Ikuhara, L. Chen, X. Huang, *Nat. Commun.* **2013**, *4*, 1870.
- [2] K.-T. Kim, C.-Y. Yu, C. S. Yoon, S.-J. Kim, Y.-K. Sun, S.-T. Myung, *Nano Energy* **2015**, *12*, 725.

- [3] X. Yu, H. Pan, W. Wan, C. Ma, J. Bai, Q. Meng, S. N. Ehrlich, Y. Hu, X. Yang, *Nano Lett.* **2013**, *13*, 4721.
- [4] G. Hasegawa, K. Kanamori, T. Kiyomura, H. Kurata, K. Nakanishi, T. Abe, *Adv. Energy Mater.* **2015**, *5*, n/a.
- [5] F. Zhao, P. Xue, H. Ge, L. Li, B. Wang, *J. Electrochem. Soc.* **2016**, *163*, A690.
- [6] L. Y. Yang, H. Z. Li, J. Liu, S. S. Tang, Y. K. Lu, S. T. Li, J. Min, N. Yan, M. Lei, *J. Mater. Chem. A* **2015**, *3*, 24446.
- [7] K. T. Kim, G. Ali, K. Y. Chung, H. Yashiro, Y.-K. Sun, J. Lu, K. Amine, S.-T. Myung, *Nano Lett.* **2014**, *14*, 416.
- [8] D. Wu, X. Li, B. Xu, N. Twu, L. Liu, G. Ceder, *Energy Environ. Sci.* **2015**, *8*, 195.
- [9] A. Henry, N. Louvain, O. Fontaine, L. Stievano, L. Monconduit, B. Boury, *ChemSusChem* **2016**, *9*, 264.
- [10] D. Su, S. Dou, G. Wang, *Chem. Mater.* **2015**, *27*, 6022.
- [11] C. Chen, Y. Wen, X. Hu, X. Ji, M. Yan, L. Mai, P. Hu, B. Shan, Y. Huang, *Nat. Commun.* **2015**, *6*, 6929.
- [12] J. Liu, M. N. Banis, B. Xiao, Q. Sun, A. Lushington, R. Li, J. Guo, T.-K. Sham, X. Sun, *J. Mater. Chem. A* **2015**, *3*, 24281.
- [13] C. Wu, P. Kopold, Y. Ding, P. A. van Aken, J. Maier, Y. Yu, *ACS Nano* **2015**, *9*, 6610.
- [14] L. Wu, D. Bresser, D. Buchholz, S. Passerini, *J. J. Electrochem. Soc.* **2015**, *162*, A3052.
- [15] D. Bresser, B. Oschmann, M. N. Tahir, F. Mueller, I. Lieberwirth, W. Tremel, R. Zentel, S. Passerini, *J. Electrochem. Soc.* **2015**, *162*, A3013.
- [16] J. Yang, H. Wang, P. Hu, J. Qi, L. Guo, L. Wang, *Small* **2015**, *11*, 3744.
- [17] Z. Wang, L. Qie, L. Yuan, W. Zhang, X. Hu, Y. Huang, *Carbon* **2013**, *55*, 328.
- [18] H. Wang, Z. Wu, F. Meng, D. Ma, X. Huang, L. Wang, X. Zhang, *ChemSusChem* **2013**, *6*, 56.
- [19] L. Fu, K. Tang, K. Song, P. A. Aken, Y. Yu, J. Maier, *Nanoscale* **2014**, *6*, 1384.
- [20] H. Song, N. Li, H. Cui, C. Wang, *Nano Energy* **2014**, *4*, 81.
- [21] J. Ding, H. Wang, Z. Li, A. Kohandehghan, K. Cui, Z. Xu, B. Zahiri, X. Tan, E. Lotfabad, B. C. Olsen, D. Mitlin, *ACS Nano* **2013**, *12*, 11004.
- [22] Y. Shao, J. Xiao, W. Wang, M. Engelhard, X. Nie, M. Gu, L. V. Saraf, G. Exarhos, J. Zhang, J. Liu, *Nano Lett.* **2013**, *13*, 3909.
- [23] X. Wang, G. Li, F. Hassan, J. Li, X. Fan, R. Batmaz, X. Xiao, Z. Chen, *Nano Energy* **2015**, *15*, 746.
- [24] K. Zhang , X. Li, J. Liang, Y. Zhu, L. Hu, Q. Cheng, C. Guo, N. Lin, Y. Qian, *Electrochim. Acta* **2015**, *155*, 174.
- [25] J. Zhu, C. Chen, Y. Lu, Y. Ge, H. Jiang, K. Fu, X. Zhang, *Carbon* **2015**, *94*, 189.
- [26] Z. Guan, H. Liu, B. Xu, X. Hao, Z. Wang, L. Chen, *J. Mater. Chem. A* **2015**, *3*, 7849.
- [27] F. Yang, Z. Zhang, K. Du, X. Zhao, W. Chen, Y. Lai, J. Li, *Carbon* **2015**, *91*, 88.
- [28] Y. Wen, K. He, Y. Zhu, F. Han, Y. Xu, I. Matsuda, Y. Ishii, J. Cumings, C. Wang, *Nat. Commun.* **2014**, *5*, 4033.
- [29] D. Xu, C. Chen, J. Xie, B. Zhang, L. Miao, J. Cai, Y. Huang, L. Zhang, *Adv. Energy Mater.* **2016**, DOI: 10.1002/aenm.201501929.
- [30] Y. Kim, Y. Park, A. Choi, N. S. Choi, J. Kim, J. Lee, J. H. Ryu, S. M. Oh, K. T. Lee, *Adv. Mater.* **2013**, *25*, 3045.
- [31] J. Qian, X. Wu, Y. Cao, X. Ai, H. Yang, *Angew. Chem.* **2013**, *125*, 4731.

- [32] J. Song, Z. Yu, M. L. Gordin, S. Hu, R. Yi, D. Tang, T. Walter, M. Regula, D. Choi, X. Li, *Nano Lett.* **2014**, *14*, 6329.
- [33] J. Sun, G. Zheng, H.-W. Lee, N. Liu, H. Wang, H. Yao, W. Yang, Y. Cui, *Nano Lett.* **2014**, *14*, 4573.
- [34] L. Pei, Q. Zhao, C. Chen, J. Liang, J. Chen, *ChemElectroChem* **2015**, *2*, 1652.
- [35] J. Qian, Y. Xiong, Y. Cao, X. Ai, H. Yang, *Nano Lett.* **2014**, *14*, 1865.
- [36] W.-J. Li, S.-L. Chou, J.-Z. Wang, H.-K. Liu, S.-X. Dou, *Chem. Commun.* **2015**, *51*, 3682.
- [37] D. Duveau, S. S. Israel, J. Fullenwarth, F. Cunin, L. Monconduit, *J. Mater. Chem. A* **2016**, *4*, 3228.
- [38] J. Liu, P. Kopold, C. Wu, P. A. van Aken, J. Maier, Y. Yu, *Energy Environ. Sci.* **2015**, *8*, 3531.